

# Driving electric field effects on the space charge limited photocurrent of $\text{In}_6\text{S}_7$

A. F. QASRAWI<sup>a,b,\*</sup>, MADLEEN A. AL-BALSHI<sup>a</sup>, N. M. GASANLY<sup>c</sup>

<sup>a</sup> Department of Physics, Arab-American University, Jenin, West Bank, Palestine

<sup>b</sup> Group of Physics, Faculty of Engineering, Atilim University, 06836 Ankara, Turkey

<sup>c</sup> Department of Physics, Middle East Technical University, 06800 Ankara, Turkey

A new type of photovoltaic materials, which are designed on the base of  $\text{In}_6\text{S}_7$  single crystals using silver and gold metals to construct  $\text{Ag}/\text{In}_6\text{S}_7/\text{Au}$  point contacted photocells, are reported and discussed. The influence of the driving electric field on the performance of the device was tested. The current density-electric field dependence curve reflected a space charge limited photocurrent effect being dominant in the field region of 1.0-4.3 V/cm. In addition, the  $\text{In}_6\text{S}_7$  photocell short circuit and loaded current dependencies on the excitation intensity were measured. The short circuit current was observed to exhibit exponential trap distribution effect and supralinear recombination at low and high illumination intensities, respectively. The device displays a current density of 0.5 mA/cm<sup>2</sup> for excitation intensity of 76 klux. When loaded, it displayed a stable power dissipation curve. Such behavior reflects the novelty of these types of cells for future application.

(Received July 23, 2012; accepted February 20, 2013)

**Keywords:** Solar energy,  $\text{In}_6\text{S}_7$ , Photo-space charge, Recombination

## 1. Introduction

Recently, the compound  $\text{In}_6\text{S}_7$  is reported to exhibit interesting characteristics that make it attractive for optoelectronic applications. Particularly, the temperature-dependent photoelectric spectra [1], the thermally stimulated photocurrent response [2], the infrared spectroscopy [3,4], the electronic structure near band edge [5], the thermoelectric power and the current conduction mechanism [6] which are investigations in this crystal reflected the ability of using this novel material for solar energy conversion and for photo-sensing as well.

Previously we have studied the dark and photocurrent properties of  $\text{Ag}/\text{In}_6\text{S}_7/\text{Ag}$  crystals in the temperature regions of 170–300 and 150–300 K, respectively [7, 8]. The dark electrical resistivity analysis which was recorded for measurements between two Ag point contacts located on the sample surface (perpendicular to the *c*-axis) has shown that the crystals exhibit intrinsic-type conduction. The data allowed the determination of the energy band gap as 0.75 eV. In contrast to this property, the photocurrent analysis revealed the existence of two photoconductivity energy levels as 0.21 and 0.10 eV, being dominant at low and high temperatures, respectively. In addition, the crystals were found to exhibit photovoltaic properties. The maximum open-circuit photovoltage and maximum short-circuit current density were found to be 0.12 V and 0.38 mA cm<sup>-2</sup>, respectively.

The main purpose of this work is to study the photovoltaic effect observed in  $\text{In}_6\text{S}_7$  with Ag-Au contacts along the crystal's *c*-axis as brilliant promising photocells. Particularly, the relation between current density and electric field in the dark and under light excitation, the electric field-photocurrent relation, the short circuit current

density and voltage open circuit dependencies on incident light intensity, and current density-voltage characteristics curves for the  $\text{Ag}/\text{In}_6\text{S}_7/\text{Au}$  will be reported and discussed. This study is expected to improve the performance of the photovoltaic device.

## 2. Experimental details

$\text{In}_6\text{S}_7$  polycrystals were synthesized from the high-purity elements (at least 99.999%) taken in stoichiometric properties. The single crystals were grown by the Bridgman method. The X-ray diffraction patterns show that these crystals have monoclinic structure with the lattice parameters  $a = 0.909$ ,  $b = 0.389$ ,  $c = 1.771$  nm and  $\beta = 108.20^\circ$ . Typical dimensions of the crystals suitable for measurements were  $3 \times 2 \times 1$  mm<sup>3</sup>. Using gold paste, point contacts were fixed at the top surface of the samples. The bottom of the samples was made of Ag contact type. The current was measured using Keithely 485 picoammeter. The voltage was supplied from a PHYWE high resolution voltage source. The illumination was done using a halogen lamp. The light intensity was calibrated using MASTECH-MS8209 radiometer.

## 3. Results and discussion

In order to understand the physical features and limitations of the newly structured  $\text{Ag}/\text{In}_6\text{S}_7/\text{Au}$  device, the current density (*J*)-electric field (*E*) characteristics were recorded in the dark and under excitation intensity of 8.8 klux. The resulting curves are displayed in Fig. 1. The figure reflects the dark *J* - *E* characteristics as empty

circles and the illuminated ones as filled circles. As the figure displays the device exhibited linear current density – electric field characteristics that reveal a dark conductivity value of  $1.02 \times 10^{-2} (\Omega\text{cm}^{-1})$ . This value, which is measured perpendicular to the sample surface (along the crystal  $c$ -axis) is much higher than that we have previously reported as  $5.52 \times 10^{-5} (\Omega\text{cm}^{-1})$  for the same crystal [7, 8]. The comparison of the present and the latter data, which corresponds to measurement along the surface of the sample (perpendicular to the crystal  $c$ -axis), reflect the high crystal anisotropy. The  $\text{In}_6\text{S}_7$  crystals are expected to be highly anisotropic due to the crystallography nature of the system. The crystal structure consists basically of two separate sections. Both of which are of almost cubic close-packed arrays of S atoms with In atoms in octahedral coordination, the two sections exhibit equivalent directions at  $61.5^\circ$  to each other [9]. Such connection causes high anisotropy.

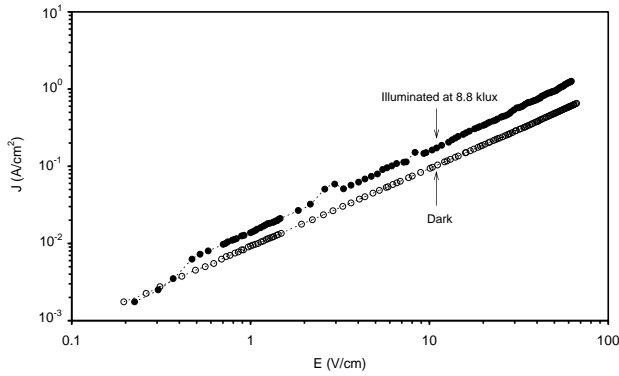


Fig. 1. The current density–applied electric field characteristics for  $\text{Ag}/\text{In}_6\text{S}_7/\text{Au}$  device. The dark  $J - E$  is shown by empty circles (o) while the illuminated ones is shown as filled circles (●).

The illuminated current density apparent in Fig. 1, increases systematically with increasing electric field for electric field values greater than 0.47 V/cm, below this value photoexcitation is not pronounced. The difference in the value of dark and photocurrent density is mainly due to the electron-hole pair generation by photoexcitation [8]. The illuminated current density–electric field dependence is also linear with conductivity value of  $2.11 \times 10^{-2} (\Omega\text{cm}^{-1})$ . The difference between illuminated and dark current densities under the influence of electric field, which is known as the photocurrent density ( $J_{ph}$ ), is displayed in Fig. 2. The  $J_{ph}$  – applied electric field dependence is plotted on a logarithmic scale to allow observation of possible non-linear variations. The  $J_{ph} - E$  dependence displayed in Fig. 2 reflects three distinguishable regions. Namely, the low applied electric field region (2.0–4.3 V/cm), in which the photocurrent depends on the square of the applied electric field, the moderate electric field region (4.4–10 V/cm), in which the power dependence is one and half and the high field region (above 10 V/cm) where  $J_{ph}$  linearly vary with  $E$ .

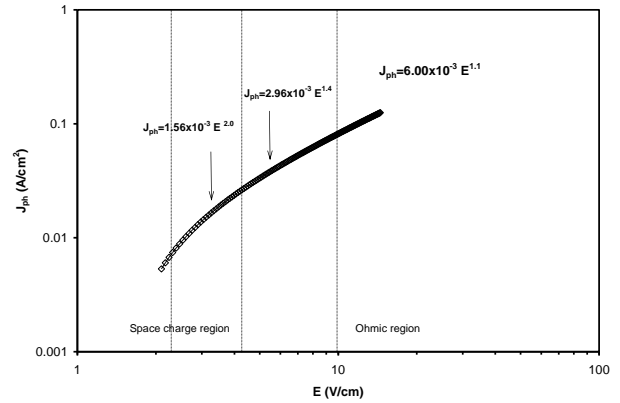


Fig. 2. The applied electric field dependence of the photocurrent for  $\text{Ag}/\text{In}_6\text{S}_7/\text{Au}$  device.

The behavior of  $J_{ph} - E$  dependence may be explained by the Mott-Gurney law in which the photocurrent density is given by [10, 11],

$$E = \sqrt{\frac{8J_{ph}}{9\epsilon\mu d^2}} \left\{ \left( d + \frac{J_{ph}\epsilon}{2N^2q^2\mu} \right)^{3/2} - \left( \frac{J_{ph}\epsilon}{2N^2q^2\mu} \right)^{3/2} \right\} \quad (1)$$

Here,  $d$ ,  $\epsilon$ ,  $\mu$  and  $N$  are being the device length, the permittivity, the mobility and the charge density close to the contact. Approximating and re-arranging this equation as reported in Ref. 10, reflects two pronounced behavior of photocurrent density with electric field. The first is known as bulk limited conduction for which the charge density near the injecting contact is high such that the device length is much greater than the charge diffusion length,  $d \gg J_{ph}\epsilon / (2N^2q^2\mu)$ , causing a space charge limited region in which  $J_{ph} \propto E^2$ . The second is known as contact limited conduction for which  $d \ll J_{ph}\epsilon / (2N^2q^2\mu)$  leading to Ohmic behavior of photocurrent density with electric field ( $J_{ph} = Nq\mu E$ ). For the case where the space charge affects the current flow but not clamping it, that is, the current is not entirely injection limited nor it is bulk limited, the electric field will affect the photocurrent density through the relation,

$$E = \frac{J_{ph}}{Nq\mu} + \frac{27Nqd}{128\epsilon}$$

N. Tessler and N. Rappaport [11] have considered the role of these regimes on the photocurrent efficiency at low and high photoexcitation rates. In the light of their analysis, the behavior of the photocurrent can be predicted as follows; at low excitation intensities the device driven current density is resembled by barrier reduction causing the device to work on the space charge limited regime. The

onset of the space charge reduces the photocurrent efficiency.

Fig. 3 reflects the short circuit current density as a function of illumination intensity ( $F$ ) being recorded from non-injected contacts. Here, no external electric field is applied. The device works as a photovoltaic cell in the light intensity region from sunrise and sunset to bright sunlight. One may notice from the figure that the resulting maximum obtainable current density is  $0.5 \text{ mA/cm}^2$  recorded at 76 klux. The value is higher than we have previously reported as  $0.35 \text{ mA/cm}^2$  recorded at  $\sim 100 \text{ klux}$  for measurement along the sample surface [8]. The plot of  $J_{sc} - F$  follows a power law of 0.9 at low illumination intensity ( $< 3.2 \text{ klux}$ ). As intensity increases, the power dependence of  $J_{sc} - F$  falls to  $\sim 0.5$  for moderate values of intensity and re-increases to 1.3 moderate at high applied illumination intensity. The latter value is very close to that we have reported for  $J_{sc} - F$  curve being recorded along the sample surface. These values provide information about the recombination kinetics of the carriers in the  $\text{In}_6\text{S}_7$  single crystals. The details of the recombination mechanism were previously reported [8] to be governed by the exchange in role between the recombination and trapping centers in the crystal. The supralinear recombination was also assigned to the strong recombination at the sample surface [12].

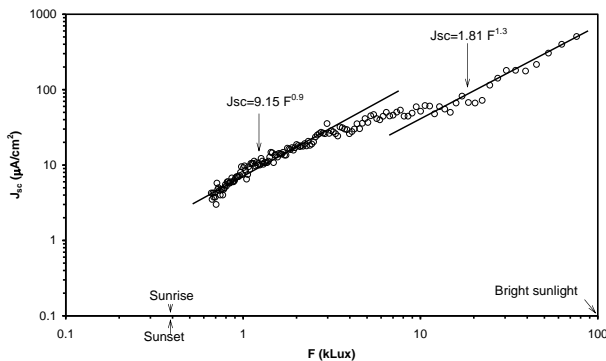


Fig. 3. The variation of the short circuit current density with the illumination intensity for the  $\text{Ag}/\text{In}_6\text{S}_7/\text{Au}$  solar cells.

Fig. 4 illustrates the  $J - V$  plot of the  $\text{Ag}/\text{In}_6\text{S}_7/\text{Au}$  photocell being recorded for different load resistances. For the displayed curve the light intensity was 1.2 klux. As one may depict from the figure, the current density tends to remain constant  $\sim 15 \text{ } (\mu\text{A}/\text{cm}^2)$  while load voltage is increased. The constant value of current density with voltage in  $\text{Ag}/\text{In}_6\text{S}_7/\text{Au}$  sample indicates that the difference between the accepted and dissipated energies is sufficient to allow charge carriers to exceed the build in electric field in the device. Unfortunately, the stability of the loaded power curves was not obtainable for all levels of irradiation. The higher the light intensity, the less stable

the power dissipation. For this reason, the research must continue on this type of photovoltaic cells to improve their performance and enlarge the output power.

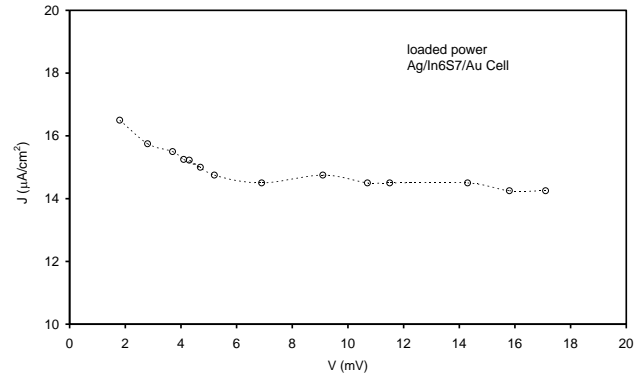


Fig. 4. The current of the cells as a function of voltage for the cell under varied load resistance.

#### 4. Conclusions

In this work the electric field and light excitation effects on the current density of  $\text{Ag}/\text{In}_6\text{S}_7/\text{Au}$  devices were studied. It was found that although the current density-electric field characteristics are linear in the dark and under illumination, the resulting photocurrent density is space charge limited. The space charge, which is associated by the exponential trap distribution, affected the recombination kinetics of the device. A high short circuit and low voltage current density were obtained for this type of solar converters. A high stability of cell current density for low load voltages was obtained. The small size of the cell, the stability of the current density, the low light intensity working ability are promising features of the  $\text{Ag}/\text{In}_6\text{S}_7/\text{Au}$  cells to be implanted in technology as micro- and nano-device electrical sources.

#### Acknowledgments

We would like to give our great thanks to the Arab American University Research fund for the financial support (Project No: 10-11 Cycle I (II)) of this investigation.

#### References

- [1] N. P. Gavaleshko, M. S. Kitsa, A. I. Savchuk, R. N. Simchuk, *Sov. Phys. Semicond.* **14**, 822 (1980).
- [2] M. Isik, N. M. Gasanly, *Phys. B: Condens. Matt.* **406**, 2650 (2011).
- [3] C. H. Ho, Y. P. Wang, Y. S. Huang, *Appl. Phys. Lett.* **100**, 131905 (2012).
- [4] N. M. Gasanly, B. M. Dzhabadov, A. S. Ragimov, V. I. Tagirov, R. E. Guseinov, *Phys. Stat. Sol. (b)* **106**, K47 (1981).

- [5] H. Ben Abdallah, R. Bennaceur, *Phys. B: Condens. Matt.* **404**, 194 (2009).
- [6] G. A. Gamal, *Cryst. Res. Technol.* **32**, 723 (1997).
- [7] A. F. Qasrawi, N. M. Gasanly, *J. All. Comp.* **426**, 64 (2006).
- [8] A. F. Qasrawi, N. M. Gasanly, *J. Phys.: Condens. Matt.* **18**, 4609 (2006).
- [9] J. H. C. Hogg, W. J. Duffin, *Acta Crystallographica* **23**, 111 (1967).
- [10] N. F. Mott, R. W. Gurney, *Electronic processes in ionic crystals*, Oxford University Press, London, 1940.
- [11] N. Tessler, N. Rappaport, *Appl. Phys. Lett.* **89**, 013504 (2006).
- [12] R. H. Bube, *Photoelectronic properties of semiconductors* (Cambridge: Cambridge University Press) 1992, pp. 59, 72, 8.

---

\*Corresponding author: aqasrawi@aaup.edu,  
aqasrawi@atilim.edu.tr